

# Transmittance of upwelling radiance at the sea surface measured in the field

Jianwei Wei<sup>\*a</sup>, Zhongping Lee<sup>a</sup>, Nima Pahlevan<sup>b,c</sup>, Marlon Lewis<sup>d</sup>

<sup>a</sup>School for the Environment, University of Massachusetts Boston, 100 Morrissey Blvd, Boston, MA 02125; <sup>b</sup>NASA Goddard Space Flight Center, 8800 Greenbelt Road, Greenbelt, MD 20771, USA;

<sup>c</sup>Sigma Space Corporation, 4600 Forbes Boulevard, Lanham, MD 20706, USA; <sup>d</sup>Department of Oceanography, Dalhousie University, 1344 Oxford Street, Halifax, NS, B3H 4J1, Canada

## ABSTRACT

The transmittance of upwelling radiance at the air-water interface is a critical quantity in ocean color remote sensing and is usually approximated as a constant ( $\sim 0.54$ ) for nadir-viewing geometries. Despite its important role, the radiance transmittance has never been measured and validated. In this paper, we present direct measurements of the spectral radiance transmittance in calm seas. The measurements were obtained by a customized instrument package equipped with two collocated radiometers. One radiometer measures the upwelling radiance just below the surface ( $L_u(0^-)$ ) while the other one directly records the water-leaving radiance ( $L_w$ ) simultaneously. The ratio of measured  $L_w$  to  $L_u(0^-)$  provides the transmittance. Our analyses suggest that the transmittance remains constant within ultraviolet and visible domain (350–700 nm) and is generally consistent with the theoretical approximations. In particular, the observed transmittance is within  $\pm 10\%$  of the theoretical value for most portions of the spectral bands (350–600 nm). Within the red portion of the spectrum, the deviations are larger but are still less than 20%. The field observations suggest an optical closure is reached.

**Keywords:** Transmittance, upwelling radiance, water-leaving radiance, optical closure, remote sensing, ocean color

## 1. INTRODUCTION

The water-leaving radiance ( $L_w$ ,  $\mu\text{Wcm}^{-2}\text{sr}^{-1}\text{nm}^{-1}$ ) emerging from the ocean carries important optical signatures of the water constituents and is fundamental for ocean color remote sensing [1]. The water-leaving radiance is propagated from the upwelling radiance right below the water surface ( $L_u(0^-)$ ,  $\mu\text{Wcm}^{-2}\text{sr}^{-1}\text{nm}^{-1}$ ), and follows the so-called radiance  $n^2$  law [2]

$$L_w = L_u(0^-) \frac{1-\rho}{n_w^2} \quad (1)$$

Here  $\rho$  is the air-sea surface reflectance for upward radiance and  $n_w$  is the refractive index of seawater. These parameters are generally treated as constants ( $\rho = 0.025$ ,  $n_w = 1.34$ ) [e.g. 3], and henceforth  $L_w = 0.54 L_u(0^-)$ . This simplified formulation of Eq. (1) is widely used in the studies of optical oceanography, including optical modeling and ocean color sea-truth exercises, etc. However, it has never been directly measured in the field.

In radiative transfer, the ratio of  $L_w$  to  $L_u(0^-)$  is known as the radiance transmittance (from below the water surface) [4]. It can be operationally defined as [5],

$$\tau(\lambda, \theta, \varphi \in \Omega_{FOV}) = \frac{L_w(0^+, \lambda, \theta, \varphi \in \Omega_{FOV})}{L_u(0^-, \lambda, \theta, \varphi \in \Omega_u)} \quad (2)$$

with transmittance  $\tau$  a nondimensional factor represented as the ratio of  $L_w$  measured by a radiometer of solid angle  $\Omega_{FOV}$  to  $L_u$  measured by a radiometer of solid angle  $\Omega_u$ . According to Eq. (2),  $\tau$  varies with viewing directions, sea surface roughness, the field of view (FOV) of the radiometers and possibly the sky radiance distribution and wavelengths. It is not an inherent optical property of the water medium.

\* jianwei.wei@umb.edu; phone: +1 617 2877396; fax: +1 617 2877474.

In this study, for the first time both  $L_w$  and  $L_u(0)$  were measured simultaneously in the field using a collocated hyperspectral radiometer suite. The measured radiance transmittance (350-700 nm) is presented and compared to theoretical predictions.

## 2. EXPERIMENTS AND DATA PROCESSING

### 2.1 Environments of Massachusetts Bay

Massachusetts Bay is a semi-enclosed embayment bordering lands to the north, west and south and adjoining the Stellwagen Bank in the east. It is one of the most studied regions at the west boundary of Gulf of Maine. On November 16, 2013, a cruise was carried out along an east-west transect extending from Boston Harbor to Stellwagen Bank. Radiometric properties were measured at four stations (Figure 1), where water depths vary between 30-60 m. Although there is significant river discharge into Boston Harbor, these stations are characteristic of green water color. The water surface was calm during the experiment (Table 1). At two stations (Station 8 and 10), we observed crystal-clear skies. For other stations, the sky was either overcast or occupied with an opaque thin layer of clouds. With regard to the air-water boundary conditions, this experimentation represents some of the most ideal environmental conditions.

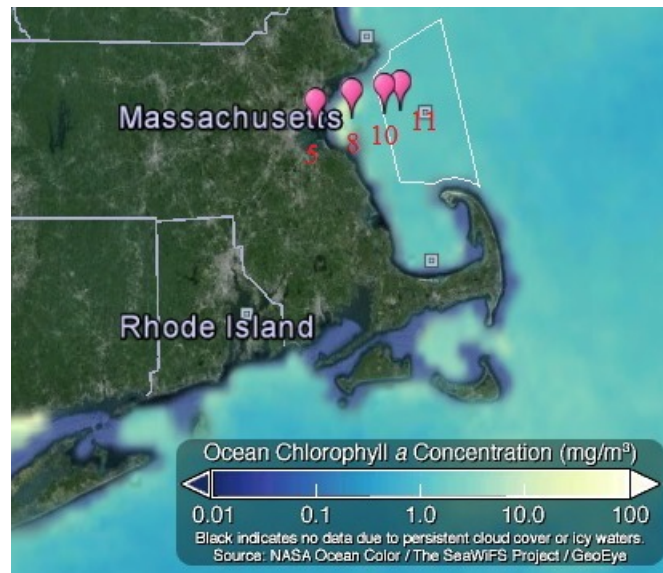


Figure 1. Stations of field experiment in Massachusetts Bay on November 16, 2013.

Table 1. Field experiment information in Massachusetts Bay.

Station No.	Depth [m]	Observation time (UTC)	Wind speed* [m/s]	Wave height* $H_{s,}$ [m]	Sky condition	Solar zenith [deg]
5	30	2013-11-16 14:50	3.9	0.32	Overcast	66
11	40	2013-11-16 16:31	2.0	0.27	Thin cloud	61
10	50	2013-11-16 17:57	0.5	0.25	Clear	64
8	30	2013-11-16 19:35	1.4	0.26	Clear	72

\* Wind speed and wave data are accessible at [http://www.ndbc.noaa.gov/station\\_history.php?station=44013](http://www.ndbc.noaa.gov/station_history.php?station=44013).

## 2.2 Collocated measurements of $L_w$ and $L_u(0)$

Two hyperspectral ocean color radiometers (HyperOCR, Satlantic LP.) were configured to measure the water-leaving radiance and in-water upwelling radiance. The HyperOCR sensors are fully digital optical packages. They have an FOV of  $3^\circ$  in air ( $8.5^\circ$  in water). The radiance can be measured at about 3 nm increments from ultraviolet (UV) to near-infrared (NIR) bands with a wavelength accuracy of  $\pm 0.1$  nm. And each spectral band is approximately 10 nm wide.

The two radiance radiometers were installed on the two fins of a HyperPRO profiler. Two sensors both looked downward and recorded the radiance at almost the same time (time difference less than 0.02 s). Differently, one radiometer measured  $L_w$  while the other one measured  $L_u(0)$ . The  $L_w$  radiometer (Serial number: HPL343) was operated according to the strategy of skylight-blocked approach (SBA) [6]. A customized cone was attached to the  $L_w$  radiometer (housing diameter 6 cm) with its open end (10 cm in diameter) immersed just below the water surface, while the radiometer window remains in the air, such that the surface-reflected light is blocked off the FOV of the radiometer. This radiometer has 137 wavelengths between 350 nm and 805 nm, and was calibrated with the National Institute of Standards and Technology (NIST) traceable standards by its manufacturer.

The upwelling radiance right below water surface was measured with another HyperOCR radiometer (Serial number: HPL191). It is equipped with 255 channels from 306 nm to 1153 nm. In operation, the  $L_u$  sensor head was immersed in the water to a nominal depth of 15 cm. Additional inter-calibration of the radiometers were implemented and are presented in Section 2.3.

During the field deployment, this instrument package was kept at least 30 meters away from the vessel in order to minimize the shadowing effect of the ship, or reflections from the hull.

## 2.3 Instrument performance testing

Inter-comparisons of the two radiance sensors were done in two days (August 5 and August 12, 2013), when the skies were sunny and clear as a quality control. The radiance instruments were placed side by side to simultaneously measure the light reflected off a standard gray card (18% reflectance). A total of fifteen data sequences were collected. The ratios of measurements by the  $L_w$  sensor to measurements by the  $L_u$  sensor are presented in Figure 2. It is found that the  $L_u$  sensor performs equivalently well ( $\pm 5\%$ ) as the  $L_w$  radiometer from the UV bands to NIR bands. This performance measure is independent of the calibration of the radiometers. The factory radiometric calibration (and the application of the immersion coefficient for the in-water sensor) was used for subsequent data analyses.

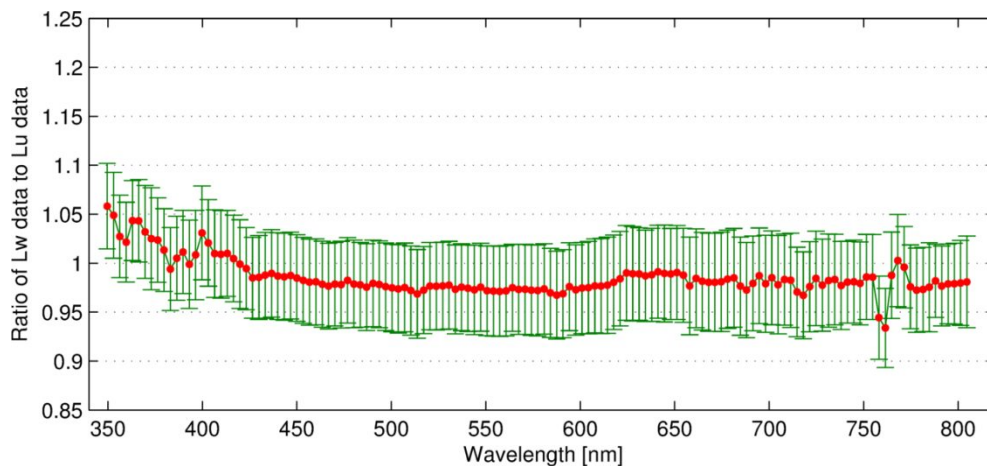


Figure 2. Measurement ratios of  $L_w$  instrument and  $L_u$  instrument. The mean values (denoted in dots) and standard deviations are illustrated.

## 2.4 Data analyses

### (a) Calibration

Level-2 radiometric data were processed and obtained using Satlantic's Prosoft data processing software. Dark values were taken every five samples by use of an internal shutter. These measurements were linearly interpolated for each light value, and then subtracted from the observations. The calibration coefficients provided by the manufacturer were used. The immersion factor ( $I_f$ ) was applied to measurements by the  $L_u$  sensor. For the  $L_w$  sensor, which was configured to operate in air, no immersion effect was considered in the data processing. Linear spectral interpolation was applied to data measured by the  $L_u$  sensor in order to match the wavebands of data measured by the  $L_w$  sensor.

### (b) Measurement correction

The self-shading effect was corrected for the measured water-leaving radiance and upwelling radiance. Specifically, we retrieved the remote-sensing reflectance ( $R_{rs} = L_w/E_s$ , units:  $\text{sr}^{-1}$ , where  $E_s$  is the downwelling plane irradiance above the sea water) a few minutes before the transmittance observation with the SBA scheme [6]. From  $R_{rs}$ , the total absorption coefficient ( $a$ ,  $\text{m}^{-1}$ ) and backscattering coefficient ( $b_b$ ,  $\text{m}^{-1}$ ) were estimated from the quasi-analytic algorithm (QAA). Then the shading effects were compensated following NASA's recommended approach [7]. The instrument diameters of  $L_w$  and  $L_u$  radiometers are 0.1 m and 0.06 m, respectively. The diameter of radiance sensor window is 0.005 m.

The measured  $L_u$  data at depth  $z$  were further extrapolated to right below the water surface using the following relationship,  $L_u(0^-) = L_u(z) \cdot \exp(K_L \cdot z)$ , where  $z = 0.15$  m, and  $K_L$  is estimated by  $(a+b_b)/\cos(\theta_{sw})$ , with  $\theta_{sw} = \text{asin}(\sin(\theta_s)/1.34)$  where  $K_L$  (unit:  $\text{m}^{-1}$ ) is the diffuse attenuation coefficient for upwelling radiance,  $\theta_s$  is the solar zenith angle and  $\theta_{sw}$  is the refracted angle of the direct solar beam in-water. Optical quantities other than angles are wavelength dependent.

### (c) Data screening

The measurements of  $L_w$  and  $L_u$  with measured instrument tilts greater than  $5^\circ$  are removed from subsequent analysis.

It was observed that the cone attached to the  $L_w$  instrument can be occasionally popped out of the water surface with passing waves. Data of those moments could be contaminated due to the light reflected into the FOV from above the water surface. To remove those bad data points, we calculated the standard deviation of the radiance measurements at two wavebands of 380 nm and 715 nm, and filtered the radiance sequence for those data beyond +1 standard deviation from the mean.

Similarly, the  $L_w$  instrument window could be immersed into the water as well due to waves, but such situations rarely occur under calm sea conditions and the effects incurred on the transmittance determination are negligible.

Results of simultaneously obtained  $L_w$  and  $L_u(0^-)$  are illustrated in Figure 3. Generally,  $L_w$  and  $L_u$  spectra exhibit similar shapes from the UV domain to visible bands.

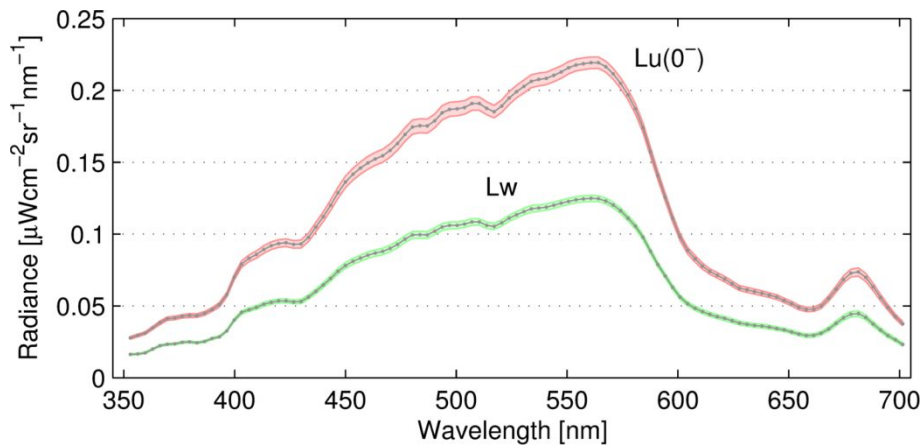


Figure 3. Measured water-leaving radiance and upwelling radiance at Station 10. The dotted line represents the mean radiance and the shaded area refers to the range of 1<sup>st</sup> standard deviation.

(d) Derivation of radiance transmittance

The instantaneous transmittance is derived as the ratio of  $L_w$  to  $L_u(0^-)$

$$\tau^i(\lambda) = \frac{L_w^i(\lambda)}{L_u^i(0^-, \lambda)} \quad (3)$$

where the superscript  $i$  denotes the  $i^{\text{th}}$  measurement of radiance. The mean value of the  $\tau^i$  data sequence is the time-averaged transmittance of the water surface for upwelling radiance.

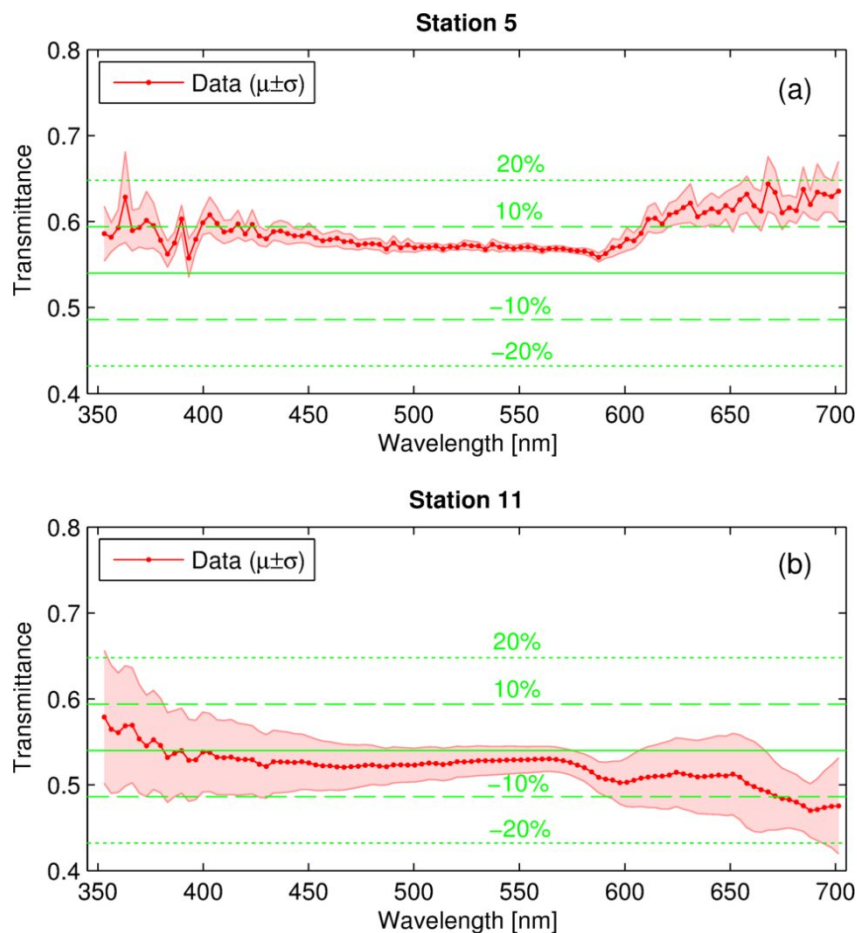


Figure 4. Spectral radiance transmittance under overcast sky (a) and opaque sky (b) The theoretical transmittance value (0.54) is denoted in solid line; the dashed lines and dotted lines represent the transmittance offset from 0.54 by  $\pm 10\%$  and  $\pm 20\%$ .

### 3. RESULTS AND DISCUSSION

Figure 4 illustrates the spectral radiance transmittance obtained at Station 5 and Station 11, where the sky was overcast and opaque, respectively. The measured transmittance at wavebands between 350 nm and 600 nm generally falls within  $\pm 10\%$  of the theoretical value. Beyond around 600 nm, the measured values go beyond the 10% error domain but still within  $\pm 20\%$  of the theoretical transmittance.

Figure 5 shows the measured transmittance for Station 10 and Station 8, where the sky was clear. Similarly, very good optical closure is found between 350 nm and 600 nm, with the absolute difference less than 10%. In the long wavebands, measured transmittance is found generally larger ( $\sim 10\text{-}20\%$ ) than the theoretically predicted values.

There are some features common in the measurements and some differences. For example, the derived transmittance is noisier at UV bands and red bands. And the results at Station 11 are slightly smaller than 0.54, while the measurements at all other stations are slightly larger than 0.54. This variability is likely relevant to the way that  $L_u(0')$  is extrapolated from  $L_u(0.1m)$ . In the data processing, the absorption and backscattering coefficients are inverted from  $R_{rs}$  spectra. Additionally, the instrument vertical displacements with waves about the  $L_u$  sensor's nominal observation depth will to some degree introduce noise to the propagation of  $L_u$  measurements. As a result, larger variability and errors may be expectable at the UV bands and red ends of the spectrum, where the light attenuates fast in Massachusetts Bay. The relatively larger deviation observed at longer wavebands is likely due to the underestimation of  $L_u(0')$  from  $L_u(z)$ . This can be further improved in the future with more accurate estimation of the total absorption coefficients and  $K_{Lu}$ .

Based on these measurements, there is no strong evidence showing spectral dependence of the transmittance for the upwelling radiance. The phytoplankton fluorescence contributes to the radiance field and is apparent with the radiance peaks around 683 nm (Figure 3). These scattering sources are currently not accounted for in our data analyses and could partly explain the relatively larger deviations of transmittance in red bands.

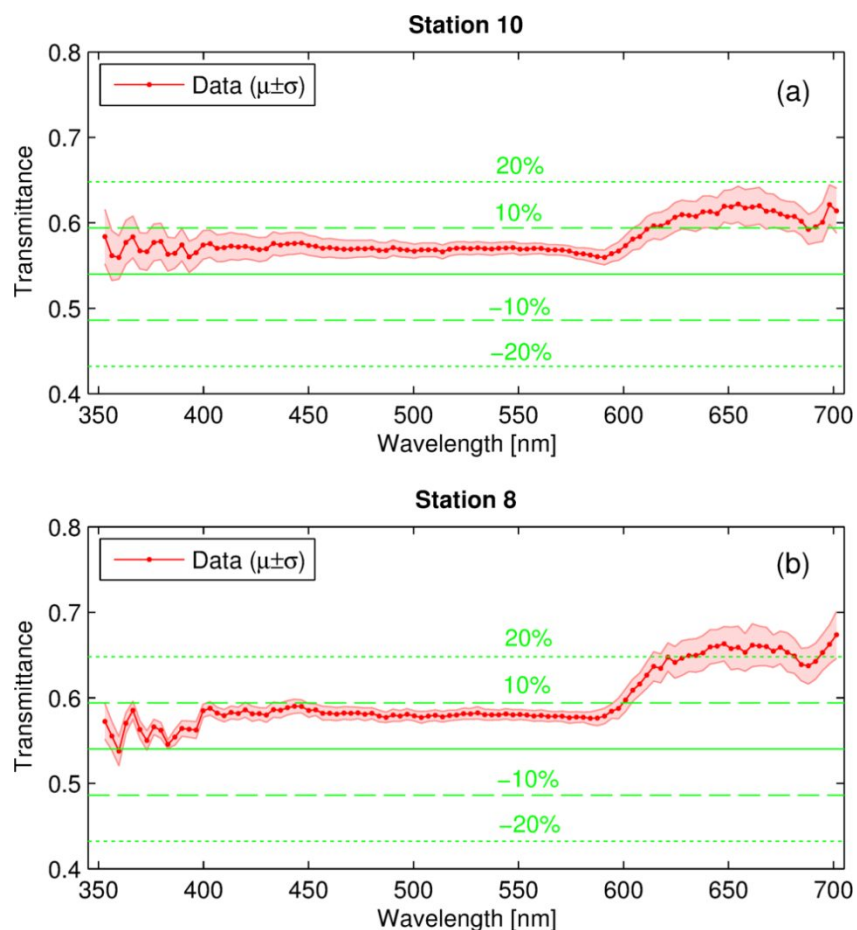


Figure 5. Spectral radiance transmittance measured under clear skies. Subplots (a) and (b) correspond to Station 10 and 8, respectively. The theoretical transmittance value (0.54) is denoted with solid line; the dashed lines and dotted lines represent the transmittance offset from 0.54 by  $\pm 10\%$  and  $\pm 20\%$ .

#### 4. CONCLUDING REMARKS

We have measured the upwelling radiance transmittance using collocated radiometers. The experiments are made in fairly calm seas. The measured radiance transmittance shows no sign of spectral dependence, and is generally in agreement with the long-adopted theoretical prediction (0.54). Although an optical closure has been reached in these measurements, it is worthwhile to continue the study of radiance transmittance in various aquatic environments and for other viewing angles. For example, the optical properties in turbid waters and clear oceanic waters can be quite different from Massachusetts Bay. Such a comprehensive study of the spectral radiance transmittance is now underway.

#### 5. ACKNOWLEDGEMENTS

We thank the support of the National Aeronautic and Space Administration (NASA) Ocean Biology and Biogeochemistry and Water and Energy Cycle Programs and the National Oceanic and Atmospheric Administration (NOAA) JPSS VIIRS Ocean Color Cal/Val Project. The University of Massachusetts Boston President's Office Funds supported the field cruise.

#### REFERENCES

- [1] H. R. Gordon, and A. Morel, [Remote assessment of ocean color for interpretation of satellite visible imagery: a review] Springer-Verlag, New York(1983).
- [2] C. D. Mobley, [Light and Water: Radiative Transfer in Natural Waters] Academic Press, Inc., San Diego, California(1994).
- [3] A. Morel, "In-water and remote measurements of ocean color," *Boundary-layer meteorology*, 18(2), 177 (1980).
- [4] R. W. Austin, [The remote sensing of spectral radiance from below the ocean surface] Academic Press, New York(1974).
- [5] C. D. Mobley, "Estimation of the remote-sensing reflectance from above-surface measurements," *Applied Optics*, 38(36), 7442-7455 (1999).
- [6] Z. P. Lee, N. Pahlevan, Y.-H. Ahn *et al.*, "Robust approach to directly measuring water-leaving radiance in the field," *Appl. Opt.*, 52(8), 1693-1701 (2013).
- [7] J. L. Mueller, G. S. Fargion, and C. R. McClain, [Ocean Optics Protocols for Satellite Ocean Color Sensor Validation, Revision 4] NASA, Goddard Space Flight Center, Greenbelt, MD(2003).